Original Article

Effect of low-density heterogeneities in telecobalt therapy and validation of dose calculation algorithm of a treatment planning system

Anuj Kumar, Sunil Dutt Sharma[1], A. K. Arya, Surabhi Gupta, Deepak Shrotriya

Department of Radiotherapy, S. N. Medical College, Agra, [1]Radiological Physics and Advisory Division, Bhabha Atomic Research Centre, Anushaktinagar, Mumbai, India

Received on: 15.07.11 **Review completed on: 22.08.11** **Accepted on: 09.09.11**

ABSTRACT

Telecobalt machines are still prominently used for the treatment of a variety of cancer cases in developing countries. The human body is a heterogeneous composition of variety of tissues and cavities which vary widely in their physical and radiological properties. The presence of heterogeneities in the path of telecobalt beam presents an altered dose distribution in the region of clinical interests. A computerized treatment planning system (TPS) is generally used for calculating the dose distribution in the patient. Experimental measurements were carried out in a telecobalt beam with the objectives to study the effects of low-density heterogeneities and to verify the ability of the ASHA radiotherapy TPS in predicting the altered dose distribution along the central axis and off-axis of the beam. Locally available kailwood was tested for its lung equivalence and measurements were carried out in a polymethyl methacrylate phantom by introducing lung equivalent and air gap heterogeneities. A comparison of experimentally measured and TPS calculated dose values indicates that the TPS overestimates the dose by 11.6% in lung equivalent (kailwood) heterogeneity along the central axis. Similarly, it was found that the TPS overestimates the dose by 3.9% and 5.9%, respectively, with air heterogeneity of 1.0 and 2.0 cm. While testing the adequacy of TPS in off-axis region, it was found that the TPS calculation does not indicate the widening of the beam profile in the low-density heterogeneity region. This study suggests that the effective path length based algorithm of the ASHA radiotherapy TPS is unable to achieve the recommended 3% accuracy of clinical dose calculation in heterogeneous media.

Key words: Dosimetry, heterogeneity, telecobalt, therapy, treatment planning, validation

Introduction

Telecobalt machines are prominently used for cancer treatment in developing countries.[1] World Health Organization (WHO) recognized telecobalt machine as a simple effective equipment to treat cancer and urged the health administrators and government agencies to give favorable consideration to this machine because of its obvious advantages such as relatively inexpensive, easy to maintain, and clinical utility in therapy or palliation.[2-3] Even in the era of hi-tech radiotherapy such as intensity modulated radiotherapy (IMRT) and image guided radiotherapy (IGRT), telecobalt therapy still has its place as far as beam therapy of masses of the cancer patients is concerned.[4]

The human body has a heterogeneous composition of a variety of tissues and cavities (lung, bone, teeth and air cavities), which vary widely in their physical and consequently radiological properties. Imaging modalities such as computed tomography (CT), magnetic resonance imaging (MRI), positron emission tomography (PET) and ultrasound allow us to accurately delineate the vital heterogeneous structure inside the human body. The normal dose distribution achieved in water or equivalent medium is altered in the heterogeneous medium of the human body.[5] The estimation of accurate dose distribution in heterogeneous system of human body is

Address for correspondence:
Dr. Anuj Kumar,
Department of Radiotherapy, S. N. Medical College,
Agra - 282 002, Uttar Pradesh, India.
E-mail: toaktyagi@yahoo.co.in

Access this article online

Quick Response Code:

Website: www.jmp.org.in

DOI: 10.4103/0971-6203.89967

therefore important for correlating the clinical outcome of the treatment. While planning the treatment of patients of carcinoma lung, esophagus, etc., lung heterogeneity correction becomes important to calculate the dose accurately. The estimation of the altered dose distribution in the photon beam off-axis is of immense clinical importance to avoid the lateral geographical missing of the target volume or overdosing of the critical structure, especially in the low-density region.[6-8]

AAPM Task Group 65 (TG 65)[6] states that the general principle of 3% accuracy in dose delivery with corresponding need for better than 2% accuracy in correcting the inhomogeneities is a reasonable albeit challenging goal. Don Robinson[9] examined the calculation accuracy of a treatment planning system (TPS) in the presence of inhomogeneities in simple geometries and found that the anisotropic analytical algorithm (AAA) overpredicts dose beyond low-density regions. In many cases, the deviation between the AAA and experimental results exceeded the 2% tolerance set by the AAPM TG 65. Da Rosa *et al.*[10] investigated the influence of lung heterogeneity for 15 MV photon beam and observed overdosage of about 40% and 20% in the lung calculated by AAA algorithm close to the interface of soft tissue/lung for 1 × 1 and 2 × 2 cm^2 field sizes, respectively. Most of the reports available in the literature dealing with the effect of heterogeneity are on megavoltage (MV) X-ray beams. Considering the massive use of telecobalt machine in the cancer treatment, measurement and quantification of the heterogeneity data for the telecobalt beam is essential.

CT image data are dependent on the density of the tissues and the beam energy where each image pixel is assigned a computed tomography Hounsfield Unit HU(CT). Chu *et al.*[11] measured the HU(CT) and also conducted a series of experiments to obtain the possible errors in measured HU(CT) as a function of electron density. These errors, although larger than those from diagnostic CT scanners, produce an error in dose less than 2% up to a depth of 20 cm. We verified the relative electron density from CT scan using experimentally evaluated relative electron densities at telecobalt energy.

With the use of advanced software and hardware technology, the TPS provides a technical advantage in calculating the dose distribution in a given medium. Central axis relative dose (CARD) and off-axis relative dose (OARD) were measured as a ratio of maximum measured dose to the dose at the point of measurement. Two basic approaches[6] are generally used in accounting for the effect of tissue inhomogeneity in dose distribution: (i) the CARD distribution within a homogeneous water-equivalent medium is calculated which is then transformed to the inhomogeneous medium dose distribution through the application of inhomogeneity correction factor (ICF) estimated using a technique usually based on effective path length, such as power law and equivalent tissue-air ratio (ETAR) methods, and (ii) model-based radiation transport within the heterogeneous medium such as AAA. Due to relatively faster calculation speed, effective path length based algorithm is commonly used in TPS to account for the effect of tissue heterogeneities.

Experimental studies were carried out in a telecobalt beam with the objectives to study the effects of low-density heterogeneities and to verify the ability of the ASHA Radiotherapy TPS which uses effective path length based algorithm in predicting the effect of low-density heterogeneity along the central axis and off-axis of the beam.

Materials and Methods

Phantom and the dosimeter

International Atomic Energy Agency (IAEA) TRS 398 dosimetry protocol recommends the use of water as the phantom material for dose measurement in beam therapy including telecobalt therapy.[12] However, various body tissue equivalent materials have been used for the measurement of the radiation absorbed dose.[6,9-11] Our selection criteria for the body tissue equivalent phantom material were mechanical strength, local availability, cost effectiveness and radiological properties such as HU(CT), relative electron density and mass density. Adequacy of the phantom materials used in this study was validated by deriving the relative electron density from the HU and experimentally measured relative electron density. The mass density of a phantom material was determined by measuring the mass and the volume of a small sample of the selected material.

Polymethyl methacrylate (PMMA) was used as tissue equivalent material while locally available kailwood was used as lung equivalent material. The tissue and lung equivalences of PMMA and kailwood, respectively, were tested by measuring their radiological properties. The relative electron densities of these two materials were determined by two different methods: (i) by determining the HU directly using CT scans taken in a diagnostic CT machine (Lemage supreme model no. 2137873, GE, Waukesha, Wisconsin USA) and (ii) by measuring the linear attenuation coefficient in a telecobalt beam. In the first method, a sample of size of 25 × 25 cm^2 and 2 cm thickness of these two materials were CT scanned using scanning protocol of thorax and by selecting a slice width of 5 mm. The CT scans were analyzed on the CT computer and the values of HU were recorded. The mean value of the HU measured using the CT scan [i.e. HU(CT)] was used for calculating the relative electron density using the relation

$$\text{Relative electron density} = \left[\frac{HU}{1000}\right]+1 \quad \text{.....(1)}$$

In the second method, the linear attenuation coefficients (m) of these materials were measured using a small volume ionization chamber (0.1 cc, Type 23323, PTW Freiburg, Germany) in a telecobalt unit (Theratron Phoenix, Best Medical, Canada). Schematic diagram of the experimental set-up used for the measurement of m is shown in Figure 1. For this purpose, the ionization chamber with its Co-60 build-up cap was placed at 110 cm distance from the telecobalt source and $5 \times 5\,cm^2$ field size was opened by the collimator of the telecobalt machine. Lead blocks were used to define a field size of about $2 \times 2\,cm^2$ at the plane of the ionization chamber. For the measurement of the linear attenuation coefficient of water, a locally made $25 \times 25\,cm^2$ water phantom with open top and a thin polythene sheet at the bottom was used. The readings of the ionization chamber without the phantom material and with various thicknesses of the phantom materials for 5 minutes irradiation were recorded and the linear attenuation coefficient (μ) was calculated using the relation

$$\mu = \frac{\log_e\left(N_0/N_x\right)}{x} \quad \text{.....(2)}$$

where N_0 (nC) is the reading of the electrometer without the attenuating material and N_x (nC) is the reading of the electrometer with the phantom material of thickness x cm.

The experimentally determined linear attenuation coefficient was used to calculate the HU [i.e. HU(M)] using the relation

$$HU = 1000\left[\frac{\mu_x - \mu_w}{\mu_w}\right] \quad \text{.....(3)}$$

where, μ_x is the measured linear attenuation coefficient of the phantom material of thickness x (cm) and μ_w is the measured linear attenuation coefficient of water. The experimentally measured μ's value was then used for calculating the relative electron density of the material using equation (1). The two values of relative electron density [one derived from the HU(CT) and the other from the HU(M)] of a given phantom material were compared.[13]

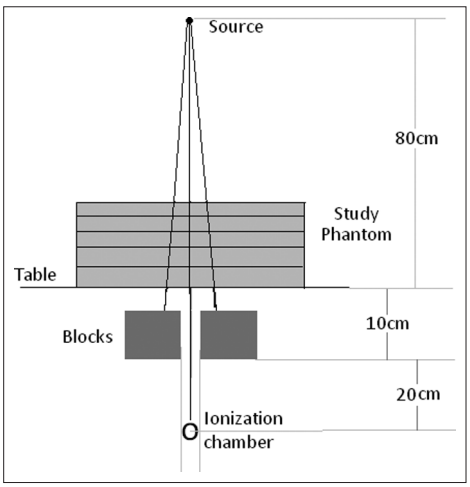

Figure 1: Schematic diagram of the experimental set-up used for the measurement of linear attenuation coefficient (μ)

Various dose measuring devices such as thermoluminescence dosimeter (TLD),[10,14,15] radiographic and radiochromic films[16,17] and ionization chamber[9,14,16,18] have been used to investigate the dose in various media. In this study, we used $0.1\,cm^3$ ionization chamber and UNIDOS electrometer (PTW Freiburg, Germany) with a valid absorbed dose to water calibration factor. Mauceri and Kase (1987) investigated the effect of mismatch of ionization chamber wall material to phantom material and demonstrated that the matching of ionization chamber wall to measuring media can be ignored provided that a small, approximately tissue-equivalent, thin-walled ($\approx 0.1\,g/cm^2$) ion chamber is used for measuring the correction factor.[19]

Experimental measurements

All the measurements were carried out in a telecobalt beam using 0° gantry angle, $5 \times 5\,cm^2$ field size and 2 minutes irradiation time. Phantom slabs of size $25 \times 25\,cm^2$ of different thicknesses were used in the experimental measurements. Totally 12 slabs of PMMA (nominal thickness 2 cm) and 7 slabs of kailwood (nominal thickness 1.8 cm) were used in the experimental measurements. Additionally, one slab (nominal thickness 2 cm) each of PMMA and kailwood having hole at its geometrical center for positioning the ionization chamber was also used. The holes at the center of the PMMA and kailwood slabs were drilled in such a way that the ionization chamber fits in exactly to minimize the air gap between the ionization chamber wall and phantom material, and hence the air gap between the ionization chamber wall and the phantom material was not taken into account while calculating the dose from the experimental measurements.

The effect of kailwood heterogeneity was studied along the central axis of the beam using phantom configuration of 5.97 cm PMMA followed by 10.94 cm lung equivalent material (kailwood) and then 7.82 cm PMMA. Clinical relevance was taken under consideration while deciding the configuration of measurement phantom. Initially, the PMMA slab containing the ionization chamber was placed at the top of the phantom and the electrometer reading for 2 minutes irradiation was recorded. The measurement depth was varied by interchanging the ionization chamber containing slab with the respective phantom slab and the electrometer readings were recorded in a similar manner. It is notable that the ionization chamber was located in the overlying PMMA phantom up to a depth of 4.94 cm, in kailwood at a depth of 4.94-15.75 cm and in underlying PMMA phantom at a depth of 15.75-25 cm. The ionization chamber was positioned in the PMMA slab

containing hole for the chamber when the measurements were carried out in overlying/underlying PMMA and the ionization chamber was positioned in the kailwood slab containing the hole for the chamber when the measurements were carried out in kailwood. This way, the measurement was carried out in the tissue overlying the kailwood heterogeneity, in the kailwood heterogeneity and in the tissue located beyond the kailwood heterogeneity. The effect of kailwood heterogeneity at off-axis was also studied by carrying out the measurements at 6.81 and 11.82 cm depths using phantom configuration of PMMA phantom up to a depth of 4.94 cm, kailwood at a depth of 4.94-15.75 cm and underlying PMMA phantom at a depth of 15.75-25 cm. These depths of measurements at off-axis were chosen to exclude the effect of electronic disequilibrium at the junction of PMMA and kailwood. For recording the electrometer reading at different off-axis points, lateral movement of the treatment table was used. A schematic diagram of the experimental set-up used for studying the effect of kailwood heterogeneity along the central axis and off-axis is shown in Figure 2.

Heterogeneity caused by the air gaps inside the human body is another case of low-density heterogeneity. To study the heterogeneity caused by air, air gaps of 1 and 2 cm were created within the PMMA slabs. Figure 3 presents the schematic diagram of experimental set-up. The electrometer readings at various depths beyond the air gap of 1 cm with a phantom configuration of 4.94 cm PMMA followed by 1 cm air gap and then 16.64 cm PMMA were recorded. The experiment was repeated in a similar manner with the air gap of 2 cm. Electrometer reading at 1.0 cm depth (overlying PMMA region) was also recorded for normalizing the dose along the central axis.

TPS calculation

The experimentally measured dose values were compared with the ASHA radiotherapy treatment planning system version 100.0 (TSG Integrations, Delhi, India) calculated dose values. The grid size used in the TPS for dose calculation was 100 × 100 points. The analytical calculation (Cunningham's algorithm) was used for the off-axis dose calculations in the TPS. The incorporation of effects of differences in tissue along the beam path is taken into account by effective path length technique. For TPS calculation of dose, the geometries similar to the dimensions of experimental set-ups [i.e. geometries of Figures 2 and 3] were defined using "define geometry" option of the TPS. The measured relative electron densities of the phantom materials were manually fed to the TPS. The phantom was irradiated selecting 0° gantry angle and 5 × 5 cm^2 field size as was done during experimental measurements. The isodose distribution was generated and the doses at different locations on the beam central axis and off-axis were recorded with the help of active cursor of the TPS. All the TPS calculation points are same as in the experimental measurement points. The CARD and OARD at a point were obtained by normalizing the dose with respect to the dose at the point corresponding to point of experimentally measured maximum dose.

Results and Discussion

The phantom materials

Table 1 presents the measured physical and radiological parameters of PMMA and kailwood. The measured data of water are also included for completeness. The measured HU(CT) of PMMA was found in the range of 98-161 with a mean value of 118.4. The HU(M) calculated from the measured linear attenuation coefficient of PMMA is 153.84. The measured values of HU for PMMA were found in good agreement with its values reported by Sharma *et al.* in 2006.[20] The HU(CT) of lung in an arbitrarily chosen CT thorax case was found to be between -900 and -500, while for kailwood, it was found to be in the range of -598 to -485 with

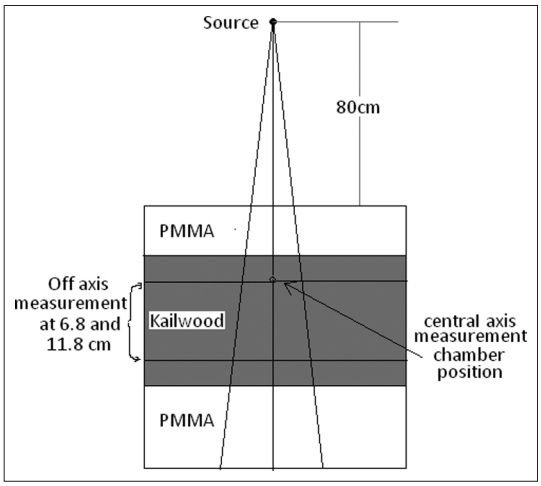

Figure 2: Schematic diagram of the experimental set-up used for studying the effect of kailwood heterogeneity in telecobalt beam along the central axis and off-axis points at depths of 6.8 and 11.8 cm

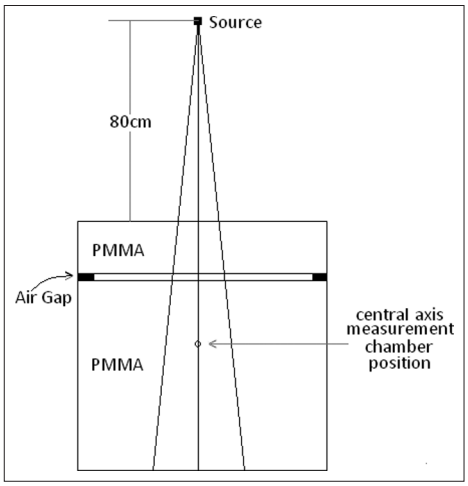

Figure 3: Schematic diagram of the experimental set-up used for studying the effect of heterogeneity caused by air gaps in the PMMA phantom in telecobalt beam

Table 1: Measured physical and radiological parameters of the PMMA, water and the kailwood

Phantom material	*Mean HU recorded from CT scan [HU(CT)]*	*Relative electron density derived from HU(CT)*	*Measured μ (cm^{-1}) in telecobalt beam*	*Mean HU measured in telecobalt beam [HU(M)]*	*Relative electron density derived from HU(M)*	*Measured mass density, p (gm/cm^3)*
PMMA	118.4	1.11	0.075	153.84	1.15	1.18
Kailwood	−511.6	0.48	0.028	−569.23	0.43	0.52
Water	1	1	0.065	-	-	-

a mean value of -511.6. The HU(M) of kailwood calculated from measured linear attenuation coefficient is -569.23. The experimentally measured values of HU and relative electron density of PMMA and kailwood were found within the range of variation of HU and relative electron density derived from the HU. Based on the measured radiological properties, PMMA was used as the tissue equivalent material and kailwood as the lung equivalent material.

CARD with kailwood heterogeneity

Figure 4 presents the measured and TPS calculated CARD in the PMMA phantom with ≈11 cm kailwood heterogeneity inside the PMMA phantom at the depth of ≈5 cm. Kailwood (M) and PMMA (M) are the dose values measured with and without kailwood heterogeneity in PMMA phantom, respectively, while kailwood (TPS) and PMMA (TPS) are the TPS calculated dose values with and without kailwood heterogeneity in PMMA phantom, respectively. While calculating the TPS values, the measured relative electron densities of PMMA (1.15) and kailwood (0.43) were taken into account. It is observed from this figure that the effect of heterogeneity is overestimated by the TPS at all the points of measurement inside the heterogeneity. The percent variation between the measured and TPS calculated values with heterogeneity shows the maximum deviation of 11.6%. However, in the absence of heterogeneity, the measured values of CARD in PMMA match with the TPS calculated values.

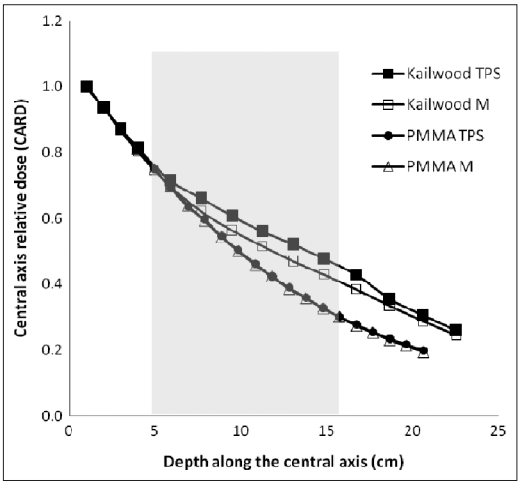

Figure 4: Measured and TPS calculated CARD of the telecobalt beam in heterogeneous phantom. CARD is the ratio of dose at a given point to the dose at 1.0 cm depth. Kailwood (M) and PMMA (M) are the dose values measured with and without kailwood heterogeneity, respectively, while kailwood (TPS) and PMMA (TPS) are the TPS calculated dose values with and without kailwood heterogeneity, respectively

Da Rosa *et al*. investigated the lung heterogeneity[7] for the narrow beam geometry using TLD and compared the measured data with various heterogeneity correction algorithms for 15 MV photon beams and for field sizes of 1 × 1, 2 × 2, 5 × 5 and 10 × 10 cm^2. They estimated overprediction of dose by the TPS in low-density medium, particularly, in narrow beam of sizes 1 × 1 and 2 × 2 cm^2. Duch[12] investigated the high-energy photon radiotherapy in lung equivalent media and found that TPS overestimated the dose inside the lung with a maximum deviation of 39% for the 18 MV photon beam for a field size of 2 × 2 cm^2. Increased transmission inside the low-density tissue increases the dose; at the same time, there is a decrease in the interaction coefficient in the low-density region.

OARD with kailwood heterogeneity

Measured and TPS calculated off-axis doses at the depths of 6.8 and 11.8 cm in heterogeneous conditions are shown in Figures 5a and 5b. Figure 5a shows the measured and TPS calculated values at 6.8 cm depth, while Figure 5b shows the measured and TPS calculated values at 11.8 cm depth. The two curves present the off-axis dose measured and calculated with kailwood heterogeneity in the PMMA phantom and without the kailwood heterogeneity in the PMMA phantom. It is observed here that the measured beam profile in the heterogeneous condition is wider in comparison to the measured profile in homogeneous condition. The electrons generated in the low-density region have wider range in comparison to the electrons generated in the PMMA. Hence, the electrons generated in low-density material deposit their energy at a relatively larger distance from the central axis of the beam in comparison to the electrons generated in the PMMA. It is also observed here that TPS, which uses the effective path length based algorithm, does not predict the elongated beam profile in heterogeneous condition, indicating that the TPS dose calculation algorithm does not account for the altered lateral dose in the low-density heterogeneity region. Tsiakalos *et al*. analyzed the penumbra enlargement[13] in lung using photon beams of 4, 6, 15 and 20 MV using films. They found the enlargement of penumbra in the middle of the low-density region. In addition, it is also observed from these two curves that the range widening of the scattered electrons in the low-density region is relatively smaller at higher depth. This would be due to the low-energy scattered electrons at the higher depth inside the low-density phantom.

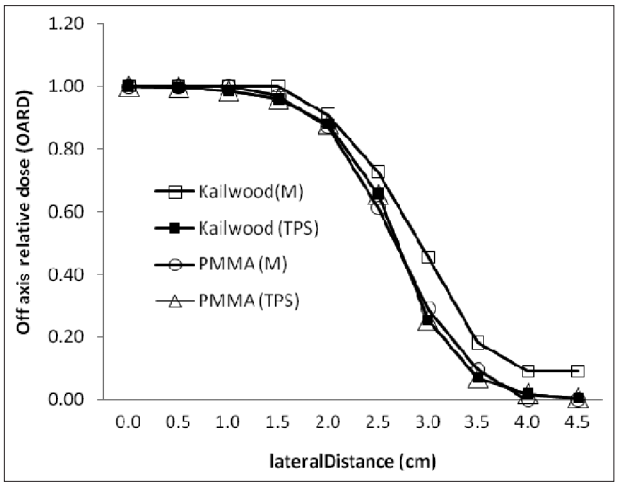

Figure 5a: Measured and TPS calculated OARD of the telecobalt beam at 6.8 cm depth. OARD here is the relative dose assuming maximum measured dose as 1 at the depth of 6.8 cm along the central axis. Kailwood (M) and kailwood (TPS) are the measured and TPS calculated OARDs, respectively, with wood heterogeneity, while PMMA (M) and PMMA (TPS) are the measured and TPS calculated OARDs, respectively, in the PMMA phantom

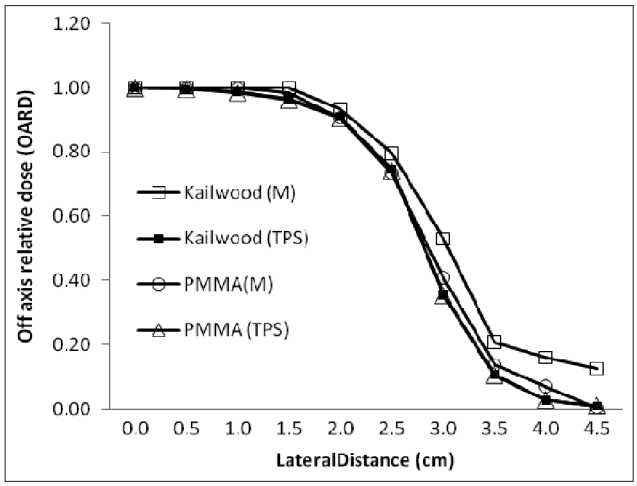

Figure 5b: Measured and TPS calculated OARD of the telecobalt beam at 11.8 cm depth. OARD here is the relative dose, assuming maximum measured dose as 1 at the depth of 11.8 cm along the central axis. Kailwood (M) and kailwood (TPS) are the measured and TPS calculated OARDs, respectively, with wood heterogeneity, while PMMA (M) and PMMA (TPS) are the measured and TPS calculated OARDs, respectively, in the PMMA phantom

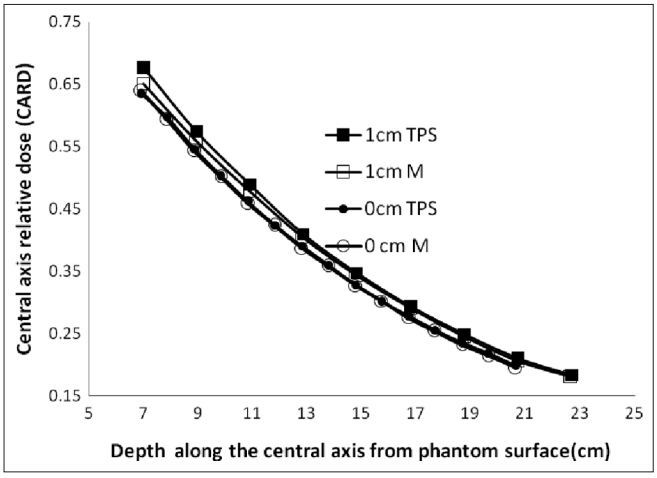

Figure 6a: Measured and TPS calculated CARD of the telecobalt beam along the central axis with 1.0 cm air cavity. 1 cm M and 1 cm TPS are the measured and TPS calculated relative doses with 1.0 cm air gap, respectively, while 0 cm M and 0 cm TPS are the measured and TPS calculated relative doses without air gap, respectively

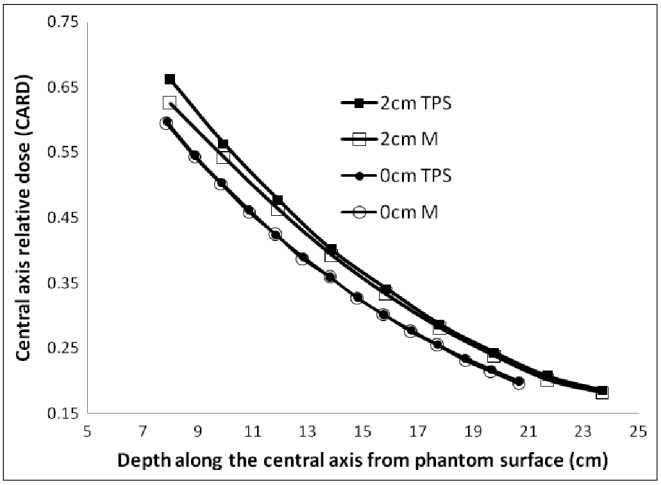

Figure 6b: Measured and TPS calculated CARD of the telecobalt beam along the central axis with 2.0 cm air cavity. 2 cm M and 2 cm TPS are the measured and TPS calculated CARDs with 2.0 cm air gap, respectively, while 0 cm M and 0 cm TPS are the measured and TPS calculated CARDs without air gap, respectively

CARD with air heterogeneity

Figures 6a and 6b present the comparison of measured and TPS calculated CARD along the central axis of the telecobalt beam with and without 1.0 and 2.0 cm air gaps, respectively. The change in relative depth dose was evaluated by comparing the data with and without air gap in the PMMA phantom. It is observed from these curves that the CARD at a given depth with air gap is higher than the CARD without air gap and the difference of CARD between these two conditions increases with increasing air gap. It is also observed that the TPS overestimated the effect of air gap in the region of 3-4 cm beyond the location of the air gap. However, TPS calculation was found to be in agreement with the measured values with air gap heterogeneity for the depths larger than 4 cm beyond the location of air gap. The maximum percentage variations in the measured and TPS calculated relative depth dose are 3.9% and 5.9% for 1.0 and 2 cm air heterogeneity, respectively. Maximum variation was found just after the air heterogeneity where the photon beam rebuilds.

Conclusions

A significant difference was found between the measured and ASHA radiotherapy TPS calculated dose values in the heterogeneous medium. In lung like low-density heterogeneity, the TPS overpredicts the dose in and beyond the low-density heterogeneity region. The source of this

overestimation of dose appears as misinterpretation of dose in the region of heterogeneity junction. The differences between the TPS calculated values and measured values are greater than the recommended acceptability criteria of 3%. The ability of ASHA radiotherapy TPS to account for the lateral effect of low-density heterogeneity was evaluated and it was found that effective path length algorithm is unable to predict the increased off-axis dose due to the well-known reason of wider range of electrons in the low-density region. Experimental results also indicated the increased off-axis dose in the low-density region.

References

1. Kumar R, Sharma SD, Phurailatpam R, Despande DD, Kannan S. Performance characteristics of indigenously developed Bhabhatron-I telecobalt unit. J Med Phys 2005;30:41-59.
2. Ravichandran R. Has the time comes for doing away with cobalt-60 teletherapy for cancer treatments? J Med Phys 2009;34:63-5.
3. World Health Organization (WHO). Optimization of radiotherapy treatment facilities. Technical report series 644, Geneva: WHO; 1980.
4. World Health Organization (WHO). Treatment of cancer. National cancer control programmes: Policies and managerial guidelines, Geneva: WHO; 1995.
5. Khan FM. The Physics of Radiation Therapy. 3rd ed. Baltimore. MD. USA: Lippincott Williams and Wilkins; 2003.
6. American Association of Physicists in Medicine (AAPM). Tissue inhomogeneity corrections for megavoltage photon beams. AAPM Report No. 85. Madison (WI): Medical Physics Publishing; 2004.
7. Jones AO, Das IJ. Comparison of inhomogeneity correction algorithms in small photon fields. Med Phys 2005;32:766-76.
8. Fogliata A, Vanetti E, Albers D, Brink C, Clivio A, Knöös T, *et al*. On the dosimetric behaviour of photon dose calculation algorithms in the presence of simple geometric heterogeneities: Comparison with Monte Carlo calculations. Phys Med Biol 2007;52:1363-85.
9. Robinson D. Inhomogeneity correction and analytic anisotropic algorithm. J Appl Clin Med Phys 2008;9:112-22.
10. da Rosa LA, Cardoso SC, Campos LT, Alves VG, Batista DV, Facure A. Percentage depth dose in heterogeneous media using thermoluminescent dosimetry. J Appl Clin Med Phys 2010;11:117-27.
11. Chu JC, Ni B, Kriz R, Saxena VA. Applications of simulator computed tomography number for photon dose calculations during radiotherapy treatment planning. Radiother Oncol 2000;55:65-73.
12. International Atomic Energy Agency (IAEA). Absorbed dose determination in external beam radiotherapy: An international code of practice for dosimetry based on standards of absorbed dose to water. Technical Report Series No. 398, Vienna: IAEA; 2000.
13. Brown S, Bailey DL, Willowson K, Baldock C. Investigation of the relationship between linear attenuation coefficients and CT Hounsfield units using radionuclides for SPECT. Appl Radiat Isotopes 2008;66:1206-12.
14. Carrasco P, Jornet N, Duch MA, Weber L, Ginjaume M, Eudaldo T, *et al*. Comparison of dose calculation algorithms in phantoms with lung heterogeneities under conditions of lateral electronic equilibrium. Med Phys 2004;31:2899-911.
15. Duch MA, Carrasco P, Ginjaume M, Jornet N, Ortega X, Ribas M. Dose evaluation in lung equivalent media in high-energy photon external radiotherapy. Radiat Prot Dosimetry 2006;120:43-7.
16. Tsiakalos MF, Theodorou K, Kappas C. Analysis of the penumbra enlargement in lung versus the quality index of photon beams: A methodology to check the dose calculation algorithm. Med Phys 2004;31:943-9.
17. Wilcox EE, Daskalov GM. Accuracy of dose measurements and calculations within and beyond heterogeneous tissues for 6 MV photon fields smaller than 4 cm produced by cyber knife. Med Phys 2008;35:2259-66.
18. Ramani R, Kohli K, Cao F, Heaton R. A dosimetric evaluation of plastic water - diagnostic- therapy (PWDT). J Appl Clin Med Phys 2008;9:98-110.
19. Mauceri T, Kase K. Effects of ionization chamber construction on dose measurements in heterogeneity. Med Phys 1987;14:653-6.
20. Sharma DS, Sharma SD, Sanu KK, Saju S, Deshpande DD, Kannan S. Performance evaluation of a dedicated computed tomography scanner used for virtual simulation using in-house fabricated CT phantoms. J Med Phys 2006;31:28-35.

How to cite this article: Kumar A, Sharma SD, Arya AK, Gupta S, Shrotriya D. Effect of low-density heterogeneities in telecobalt therapy and validation of dose calculation algorithm of a treatment planning system. J Med Phys 2011;36:198-204.
Source of Support: Nil, **Conflict of Interest:** None declared.